Pharmaceutical Research, Vol. 23, No. 10, October 2006 (© 2006)
DOI: 10.1007/s11095-006-9110-6

Research Paper

Cocrystal Formation during Cogrinding and Storage is Mediated by Amorphous Phase

Adivaraha Jayasankar,[1] Anongnat Somwangthanaroj,[1,2] Zezhi J. Shao,[3] and Naír Rodríguez-Hornedo[1,4,5]

Received January 20, 2006; accepted July 5, 2006; published online September 19, 2006

Purpose. The purpose of this work was to investigate the mechanisms of cocrystal formation during cogrinding and storage of solid reactants, and to establish the effects of water by cogrinding with hydrated form of reactants and varying RH conditions during storage.
Methods. The hydrogen bonded 1:1 carbamazepine–saccharin cocrystal (CBZ–SAC) was used as a model compound. Cogrinding of solid reactants was studied under ambient and cryogenic conditions. The anhydrous, CBZ (III), and dihydrate forms of CBZ were studied. Coground samples were stored at room temperature at 0% and 75% RH. Samples were analyzed by XRPD, FTIR and DSC.
Results. Cocrystals prepared by cogrinding and during storage were similar to those prepared by solvent methods. The rate of cocrystallization was increased by cogrinding the hydrated form of CBZ and by increasing RH during storage. Cryogenic cogrinding led to higher levels of amorphization than room temperature cogrinding. The amorphous phase exhibited a T_g around 41°C and transformed to cocrystal during storage.
Conclusions. Amorphous phases generated by pharmaceutical processes lead to cocrystal formation under conditions where there is increased molecular mobility and complementarity. Water, a potent plasticizer, enhances the rate of cocrystallization. This has powerful implications to control process induced transformations.

KEY WORDS: amorphization; cocrystal; crystallization; molecular complex; process-induced transformation.

INTRODUCTION

Hydrogen bonds are the basis of molecular recognition phenomena in biological and pharmaceutical systems. They are also key elements in the design of molecular assemblies and supermolecules in the liquid and solid states. In the crystalline state, hydrogen bonds are responsible for the generation of families of molecular networks with the same molecular components (single component crystals and their polymorphs) or with different molecular components (multiple component crystals or cocrystals) (1–12).

Cocrystals, also referred to as molecular complexes, include two or more different components and often rely on hydrogen bonded assemblies between neutral molecules. Cocrystals with the same active pharmaceutical ingredient (API) will have strikingly different pharmaceutical properties (melting point, solubility, dissolution, bioavailability, moisture uptake, chemical stability, etc.), depending on the nature of the second component (13–16). It is important to note that cocrystals are a homogeneous phase of stoichiometric composition and not a mixture of pure component crystalline phases. Key questions in the discovery of families of cocrystals are: (1) do cocrystals offer any advantages over other solid-state forms, (2) what are the criteria for cocrystal former selection, (3) can cocrystal screening and cocrystallization methods be theoretically based, and (4) can cocrystals form as a result of stresses encountered during pharmaceutical processes and storage? The research presented in this manuscript will address the last question.

Cocrystallization is a result of competing molecular associations between similar molecules, or homomers, and different molecules or heteromers (6,9,10). Most studies on cocrystal formation focus on design and isolation for the purpose of crystal structure determination, and the factors that control cocrystallization have not been explicitly considered (2,3,6,8–10,16–18). Cocrystals have therefore been prepared largely on a trial and error basis by solution, solid-state, or melt processes.

Solution-based methods in search of cocrystals have suffered from the risk of crystallizing the single component phases and often a very large number of solvents and experimental conditions need to be tested (19). Furthermore, transferability to large-scale crystallization processes has been limited. We have recently developed reaction cocrystallization

[1] Department of Pharmaceutical Sciences, University of Michigan, Ann Arbor, Michigan, USA.
[2] Present Address: Department of Chemical Engineering, Chulalongkorn University, Bangkok, Thailand.
[3] Pfizer Global Research and Development, Ann Arbor, Michigan, USA.
[4] 428 Church Street, Ann Arbor, Michigan 48109-1065, USA.
[5] To whom correspondence should be addressed. (e-mail: nrh@umich.edu)

methods where nucleation and growth of cocrystals are directed by the effect of cocrystal components on decreasing the solubility of the molecular complex to be crystallized (20,21). Thus, the success of crystallizing the molecular complex is significantly improved by varying reactant concentrations such that the supersaturation with respect to cocrystal is selectively increased.

One way to cope with the complexities of solution-based methods has been to screen for cocrystals by cogrinding solid reactants (4,6,9,17,22). Although examples of cocrystals formed by this process are abundant, the underlying mechanisms and the factors that determine cocrystallization by cogrinding are not known. Disorder induced by grinding or milling is well documented in the pharmaceutical literature and its effects on solid-state changes and reactivity have been thoroughly studied (23–28). These include amorphous phase formation, polymorphic transformations, complexation, and chemical reactivity. Therefore, the concepts of solid-state reactivity in pharmaceutical materials can be applied to understand the formation of cocrystals by solid-state methods.

Since the basis for reactivity in the solid-state lies on molecular mobility and complementarity, process-induced cocrystal formation must be related to the propensity of API and other components to form disordered or amorphous phases. That is, as long as the transformation does not occur through the melt caused by high local temperatures during a process. Cogrinding under cryogenic conditions is necessary to ascertain that the reaction does not proceed through the melt. Thus, if amorphous phases generate cocrystals, then cocrystals can form not only during the process that induced the disorder, but also during storage. Furthermore, the presence of plasticizers, such as water or other solvents that lower the T_g and enhance molecular mobility (29,30) will increase reactivity and cocrystallization rate in the solid state. To challenge these hypotheses is the focus of our work.

The objectives of the present study are to (1) investigate the underlying mechanisms of cocrystal formation during cogrinding and storage, and (2) establish the effects of water by cogrinding hydrated crystal forms of reactants and by varying RH conditions during storage. The hydrogen bonded 1:1 carbamazepine–saccharin cocrystal is chosen as a model system because its crystal structure is known (31) and it has functional groups that are commonly encountered in other pharmaceutical components. Cocrystals of carbamazepine with saccharin or nicotinamide have been shown to improve dissolution, mechanical properties, moisture uptake behavior, and chemical stability relative to the pure carbamazepine crystal, anhydrous monoclinic form III, (CBZ(III)) (14,15). Crystal structures have been reported (31) and cocrystals are prepared by solution methods (14,15) and by solid-state methods (32). We have shown that the carbamazepine –saccharin and carbamazepine–nicotinamide cocrystals can be formed from the amorphous phases generated either by quenching the melt of components (33), or by grinding a blend of components (32).

Perhaps the most relevant implication of the findings presented here, for those who are not interested in proactively searching for cocrystals, is to be able to anticipate the propensity of solid components to form cocrystals during storage as a result of the disorder created during a pharmaceutical process, such as grinding. Process induced transformations to cocrystal may thus be added to the list of transformations that can considerably affect product safety and performance in addition to transformations involving polymorphs and solvates.

MATERIALS

Anhydrous monoclinic form III carbamazepine (CBZ(III)) and saccharin (SAC) were obtained from Sigma Aldrich and were used as received. The compounds were analyzed by infrared spectroscopy (ATR-FTIR), X-ray powder diffraction (XRPD), and differential scanning calorimetry (DSC) before carrying out the experiments.

CBZ–SAC cocrystal and carbamazepine dihydrate (CBZ(D)) were prepared according to the methods described earlier (20,21,24). Solid phases were analyzed by XRPD, ATR-FTIR, DSC and thermogravimetric analysis (TGA). Experimental XRPD of the cocrystal was in agreement with that calculated using the Lorentz-polarisation correction by Mercury (ver.1.3) for the structure reported in the Cambridge Structural Database (reference code: UNEZAO).

METHODS

Cogrinding

Cogrinding was carried out at room temperature in a ball mill (5100 SPEX CertiPrep, Metuchen, NJ) and under liquid nitrogen using a cryogenic impact mill (6750 SPEX CertiPrep, Metuchen, NJ).

Room Temperature Cogrinding Methodology

Anhydrous CBZ(III) was coground with SAC, in stoichiometric (1:1) and non-stoichiometric ratios (1:2 and 2:1) in a 5100 SPEX CertiPrep Mixer/Mill using a 3114 stainless steel vial having a grinding load volume of 0.6 ml (0.5 inch diameter $\times$ 1 inch length). Two stainless steel beads about 0.25 inches in diameter were used for cogrinding. Total mass of each blend consisting of CBZ(III) and SAC was 0.5 g. Cogrinding of the blends was carried out at room temperature for different time periods up to 30 min. The temperature of the grinding vial, determined by placing a thermometer to the outside of the vial, was 45°C after 30 min of cogrinding.

Cogrinding the dihydrate form of carbamazepine, CBZ(D), with SAC in stoichiometric ratio (1:1) of reactants was carried out in the room temperature mill. Due to the low bulk density of this blend, the total mass of the blend ground was 0.25 g since the vial could not hold 0.5 g of the blend. For comparison of the rate of cocrystal formation between the dihydrate and anhydrous system, a blend of CBZ(III) and SAC weighing 0.25 g was also studied. Samples were analyzed by ATR-FTIR, XRPD, and DSC to examine changes in crystallinity and in polymorph, solvate, and cocrystal forms during cogrinding and during storage.

Cryogenic Cogrinding Methodology

Cogrinding of CBZ(III) and SAC in stoichiometric ratio was carried out in a SPEX 6750 cryogenic mill using a polycarbonate vial with 4 ml capacity. A stainless steel rod

was used as an impactor for grinding. The total mass of the blend was 1 g. The mill was programmed to an impact frequency of 10 Hz and 15 cycles, each cycle consisting of 2 min grinding followed by 2 min cooling period. Thus, the total grinding time was 30 min. The vial containing the coground sample was later transferred to a desiccator containing phosphorous pentoxide as the desiccant to allow the sample to reach room temperature, and to prevent condensation of moisture on the sample due to low temperature of the sample. Ground samples were analyzed by the methods indicated above.

Storage of Samples

The coground samples were stored in desiccators equilibrated at 0% and 75% relative humidities using phosphorous pentoxide and saturated sodium chloride solution respectively (34) at room temperature (22–25°C). XRPD and FTIR spectra of the milled blends during storage were obtained to evaluate changes in crystallinity and to monitor cocrystal formation.

Attenuated Total Reflection Fourier Transform Infra-red Spectroscopy (ATR-FTIR)

ATR-FTIR was used to identify intermolecular interactions, hydrogen bond directed molecular associations and to determine solid-state forms (polymorph, solvate, or cocrystal). The samples were analyzed using a Vertex 77 spectrometer from Bruker Optics (Billerica, MA) and a Nicolet 6700 spectrometer from Thermo Electron (Madison, WI). Both spectrometers were equipped with a DTGS detector and a single bounce ATR accessory with ZnSe crystal. Spectra (64 scans at 4 cm^{-1} resolution) were collected in the 4,000–600 cm^{-1} range.

Quantification of CBZ–SAC cocrystal formation during cogrinding and during storage was done according to IR quantitative methods reported for blends of polymorphs (35,36). Calibration curves were obtained as described below.

Calibration standards were prepared by blending CBZ(III) and SAC in 1:1 molar ratio with the required amount of CBZ–SAC cocrystal. Cocrystal used in the calibration was prepared by the solution method described previously (20,21). The total mass of each standard was 0.5 g. The standards prepared had 0, 20, 40, 60, 80 and 100 per cent (by weight) CBZ–SAC cocrystal. Samples containing 10, 50 and 90 per cent CBZ–SAC cocrystal were used as validation standards for the calibration curve.

The standards were prepared by grinding 0.5 g of each component individually for 2 to 3 min in the room temperature mill. This was done to reduce particle size differences between these components and to obtain a homogeneous blend for the standards. The three components were then weighed and blended in a stainless steel vial without the grinding beads in the SPEX 5100 mill. The samples after blending were analyzed in the Nicolet 6700 spectrometer equipped with the ATR accessory. Three samples were taken from each standard and analyzed. The spectra of the replicates collected for each standard were compared to ensure homogeneity in the standards. If the spectra of the replicates of a particular standard differed from one another, the standard was prepared again by blending for a longer time. This procedure was repeated until a homogeneous blend was obtained. The spectra collected in this manner for all the standards were then used for obtaining a calibration curve using the Partial Least Square method in the Quant software for OPUS. The calibration curve obtained was then validated using the validation standards. The R^2 values for the calibration and validation were 0.99.

X-ray Powder Diffraction (XRPD)

XRPD was used to identify crystalline phases and to qualitatively examine changes in crystallinity. Measurements were done with a Scintag X1 diffractometer (Cupertino, CA) having a copper-target X-ray tube (CuKα radiation 1.54 Å). Data were collected at a scan rate of 2.5°/min over a 2θ range of 5° to 40°. The accelerating voltage was 35 kV and the current was 20 A.

XRPD was also done using a Rigaku miniflex diffractometer (The Woodlands, TX) having a copper target X-ray tube. Data were collected at a scan rate of 2.5°/min over a 2θ range of 2.5° to 40°. The accelerating voltage was 30 kV and the current was 15 mA.

Differential Scanning Calorimetry (DSC)

Thermal analysis of samples was carried out using a TA 2590 DSC (TA instruments, New Castle, DE) which was calibrated for temperature and cell constants using indium and n-dodecane. Samples (6–8 mg) crimped in aluminum pans were analyzed in the DSC from −20 to 200°C at a heating rate of 10°C/min. Samples were continuously purged with nitrogen at 50 ml/min. Samples were also analyzed using modulated differential scanning calorimetry (MDSC) to determine the T_g of coground samples. The temperature modulation was ± 1°C with a 60 s period.

RESULTS

FTIR Spectra of Crystalline and Cocrystalline Phases

Since cocrystal formation is a result of interactions between different molecular components that also exist in the single-component crystalline states, vibrational spectroscopy is an excellent technique to characterize and study cocrystallization. Differences in hydrogen bond interactions of CBZ–SAC cocrystals and crystalline reactants (CBZ(III), CBZ(D) and SAC) shown in Fig. 1, lead to significant changes in FTIR spectra as shown in Fig. 2.

Examination of the crystal structures of CBZ(III), CBZ(D) and cocrystal CBZ–SAC (Fig. 1) shows the formation of homodimers with the CBZ carboxamide unit acting as both a hydrogen bond donor (syn-NH) and acceptor (C = O). Compared to other primary amide crystals, CBZ(III) and all anhydrous CBZ polymorphs do not posses the conventional ribbons of carboxamide dimers because the azepine ring sterically blocks the exterior amide hydrogen bond donor (anti-NH) and acceptor. This anti-NH is however involved in linking CBZ and water molecules by N–H···O hydrogen bonds as shown for CBZ(D), while maintaining the carbox-

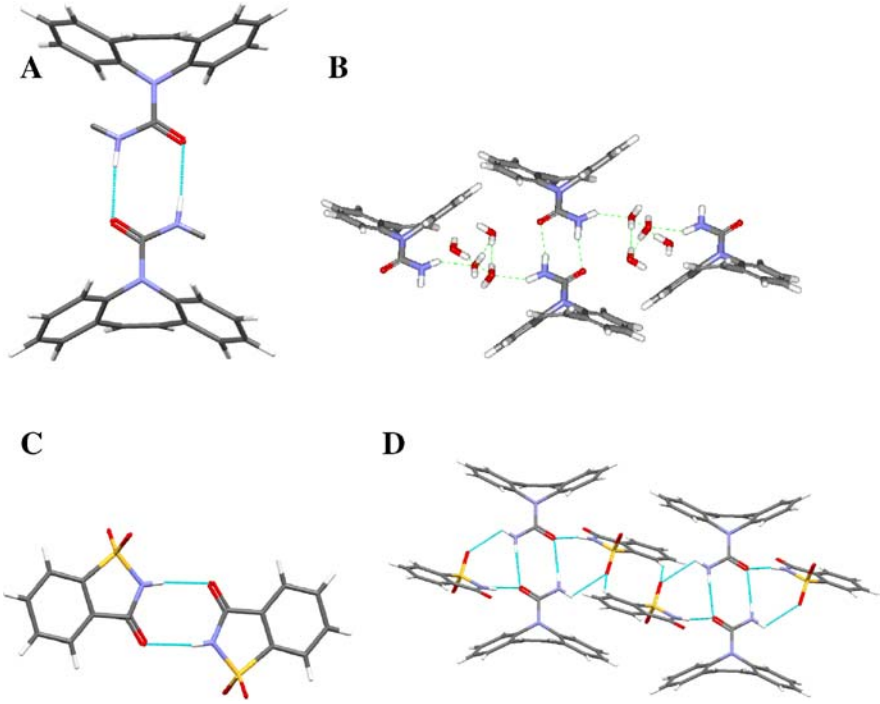

Fig. 1. Hydrogen bond interactions in crystal structures of (A) anhydrous monoclinic CBZ(III), (B) dihydrate CBZ, (C) SAC and (D) CBZ–SAC cocrystal.

amide homodimer. Similar molecular interactions are observed in the acetone and DMSO solvates of CBZ (31).

One of the strategies in designing CBZ cocrystals is to fulfill the donors and acceptors in the carboxamide dimers, by linking the anti-NH hydrogen bond donor and acceptor (C = O) sites of CBZ that are not involved in the homodimer as shown in the cocrystal of CBZ–SAC (Fig. 1) (31). In this cocrystal, saccharin forms an N–H···O = C with the carbamazepine carbonyl, and an S = O···H–N with the additional donor of the carbamazepine amide. Compared to the crystal structure of pure saccharin, homomeric N–H···O = C dimers are replaced with heteromeric N–H···O = C dimers in the cocrystal, leaving the carbonyl group in SAC free. In addition, the free SO_2 in pure SAC is engaged in weak S = O···H–N bonds with CBZ in the cocrystal and forms S = O···H–C bonds between SAC molecules (31). These differences in hydrogen bond interactions are shown in the FTIR spectra of these materials as discussed below, and were used to study cocrystallization by cogrinding solid reactants and during storage.

The IR spectrum of CBZ(III) in Fig. 2 shows peaks at 3,465 and 3,157 cm^{-1} that correspond to the free anti-NH and hydrogen bonded syn-NH respectively in CBZ(III) (37). A peak corresponding to the carbonyl stretch is observed in the spectrum at 1,676 cm^{-1} (38,39). Peaks corresponding to NH and carbonyl stretch of the amide are also observed in the spectrum of CBZ(D). A peak at 3,432 cm^{-1} for NH stretch, lower than that observed at 3,465 cm^{-1} in CBZ(III), is observed in the spectrum of CBZ(D). The shift of the peak towards lower wavenumber is due to hydrogen bonding between the free NH of CBZ and the oxygen of water (38,39). The peak corresponding to the carbonyl stretch in CBZ(D) is observed at 1,677 cm^{-1} and is similar to that observed in CBZ(III). These spectral differences reveal the hydrogen bond pattern differences between the anhydrous (III) and hydrated forms of CBZ as presented in Fig. 1.

The spectrum of pure SAC also shows peaks corresponding to NH and CO stretch of the secondary amide at 3,094 and 1,719 cm^{-1} (40–42). In addition, peaks corresponding to asymmetric and symmetric stretching of $–SO_2$ group in SAC are also observed at 1,332 and 1,175 cm^{-1} respectively (38,39,41,43).

Comparison of the spectrum of CBZ–SAC cocrystal with that of CBZ(III) and SAC (Fig. 2) shows peak shifts in the carbonyl, amide, and SO_2 regions in the cocrystal spectrum that relate to hydrogen bond interactions in their crystal structures. Peaks corresponding to free carbonyl of SAC and hydrogen bonded carbonyl of CBZ are observed at 1,726 and 1,645 cm^{-1}, respectively in the spectrum of the cocrystal (14,38,39). A peak shift is observed corresponding to NH stretch of the amide from 3,465 cm^{-1} for CBZ(III) to 3,498 cm^{-1} for the cocrystal. Comparison of the spectrum of SAC and CBZ–SAC cocrystal shows a peak shift corresponding to the asymmetric stretch of $–SO_2$ from 1,332 cm^{-1} in the spectrum of SAC to 1,327 cm^{-1} in the spectrum of the cocrystal.

Cocrystal Formation by Cogrinding Anhydrous CBZ(III) and SAC

XRPD patterns and FTIR spectra before and after cogrinding CBZ(III) and SAC equimolar blends for 30 min under ambient and cryogenic conditions are shown in Figs. 3

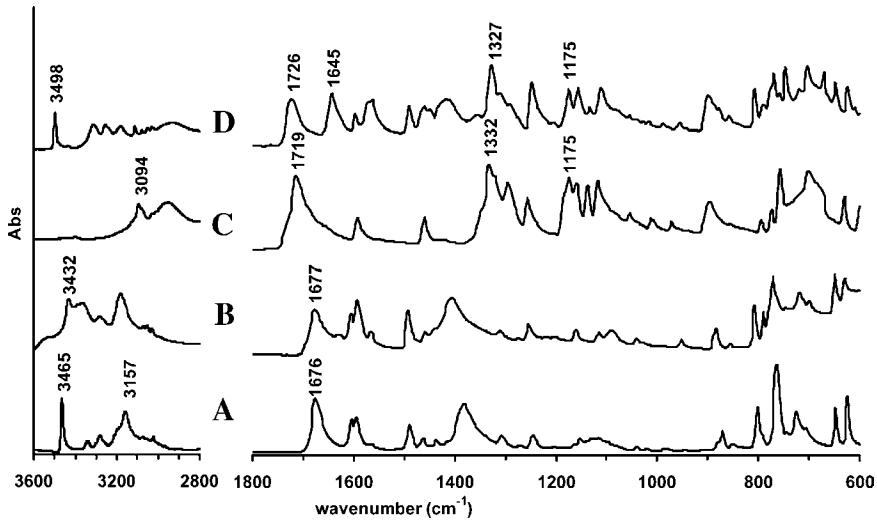

Fig. 2. Infra-red spectra of (A) CBZ(III) (B) CBZ(D) (C) SAC and (D) CBZ–SAC cocrystal prepared from solution.

and 4. A decrease in XRPD peak intensities was observed, with the decrease being greater for the blend milled under cryogenic conditions (Fig. 3). This indicates a larger reduction in the crystallinity of reactant materials under cryogenic conditions, with a few low intensity peaks that are common to cocrystal or reactants. Ambient temperature cogrinding resulted in transformation to the cocrystalline phase as indicated by the diffraction peaks at 7.0° and 28.3° unique to the CBZ–SAC cocrystal. A low intensity broad peak around 27° corresponding to CBZ and or SAC suggests the presence of unreacted crystalline material.

FTIR analysis provided information regarding the intermolecular interactions and phase transformations occurring in these processes (Fig. 4). Infrared spectra show stronger peaks corresponding to CBZ–SAC cocrystal at 3,498, 1,726 and 1,645 cm^{-1} after ambient temperature cogrinding. These observations are consistent with the XRPD analysis and suggest that hydrogen bond heteromeric associations between CBZ and SAC, similar to those in the cocrystal, occur at a faster rate during cogrinding at ambient temperature than under cryogenic conditions. Peaks characteristic of CBZ(III) and SAC are also observed, indicating some unreacted components.

Spectral shifts after cryogenic cogrinding also indicate changes in intermolecular interactions between CBZ and SAC in the XRPD disordered phase. A broad shoulder between 3,475 and 3,520 cm^{-1}, corresponding to $-NH_2$ stretch in the amide group, and spectral changes in the carbonyl stretching region that reveal changes in hydrogen bond interactions preceding complex formation are observed. Further studies of spectral shifts and chemical interpretations are currently under investigation in our laboratory.

To confirm the presence of a disordered or an amorphous phase, DSC analysis was carried out. Figure 5 shows the presence of an amorphous phase in the cryogenically

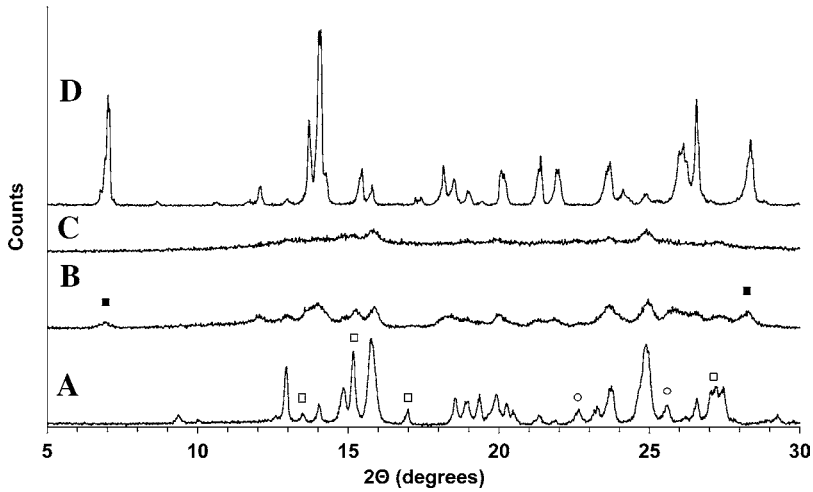

Fig. 3. XRPD patterns showing cocrystal and amorphous phase formation after 30 min room temperature and cryogenic cogrinding of CBZ(III) and SAC. (A) Before cogrinding, (B) after room temperature cogrinding, (C) after cryogenic cogrinding and (D) CBZ–SAC cocrystal prepared from solution (symbols □, ○ and ■ indicate CBZ(III), SAC and CBZ–SAC cocrystal prepared from solution).

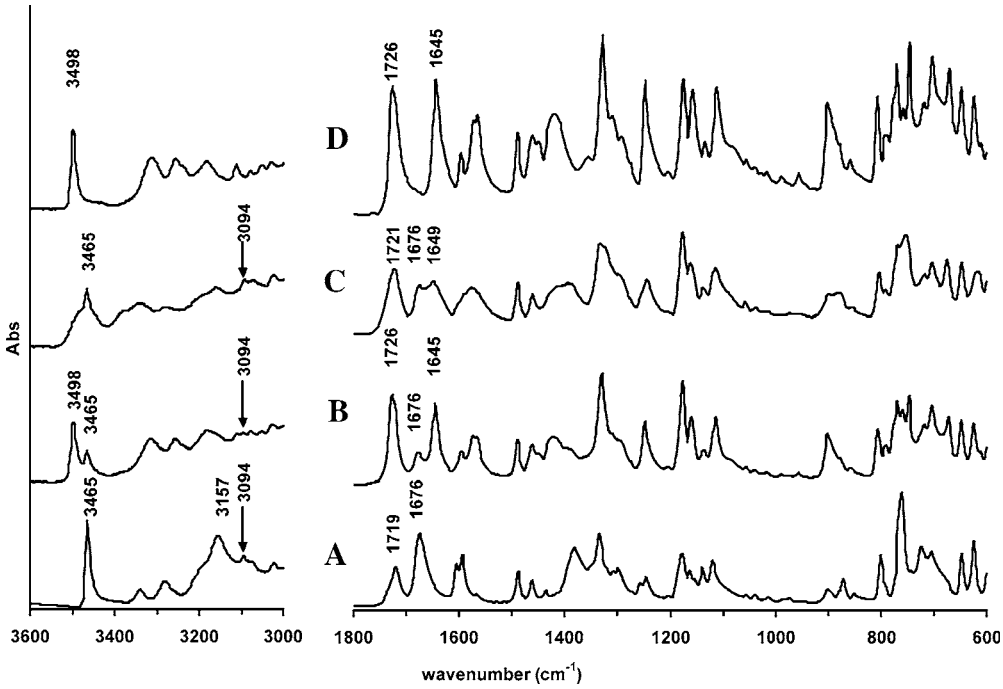

Fig. 4. Infra-red spectra showing interactions between CBZ and SAC after 30 min room temperature and cryogenic cogrinding of CBZ(III) and SAC. (A) before cogrinding, (B) after room temperature cogrinding, (C) after cryogenic cogrinding and (D) CBZ–SAC cocrystal prepared from solution.

coground sample with a T_g around 41°C, followed by a crystallization event (exotherm) around 69°C before an endotherm at 174°C that agrees with the melt of the CBZ–SAC cocrystalline phase at 176°C. XRPD analysis of the sample after the exothermic crystallization event and before the melt, shows peaks corresponding to cocrystal and a few peaks with weak intensities due to unreacted components (result not shown). The presence of unreacted components would cause a decrease in the melting point and may be the reason for the slightly lower melting points measured. Cogrinding under ambient conditions showed a single endothermic event at 174°C. Pure CBZ(III) has been reported to melt at 174 to 176°C and transform to CBZ (I) followed by the melt of form I at 189°C (44). The melting point of pure SAC was determined to be 228°C. Due to chemical degradation of CBZ, thermal analysis studies were done below 200°C.

The glass transition temperature of amorphous materials is an important property that determines molecular mobility and reactivity, and is thus considered in examining the results from cogrinding under ambient and cryogenic conditions.

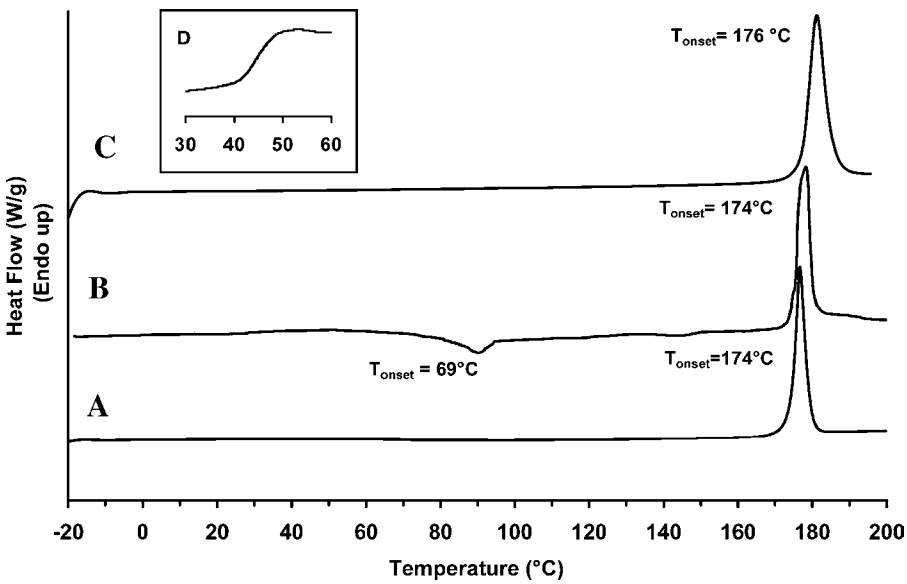

Fig. 5. DSC analysis of CBZ(III) and SAC blends after cogrinding for 30 min under the following conditions: (A) room temperature, (B) cryogenic condition, (C) CBZ–SAC cocrystal prepared from solution, and (D) inset showing the T_g determined using MDSC after cryogenic cogrinding.

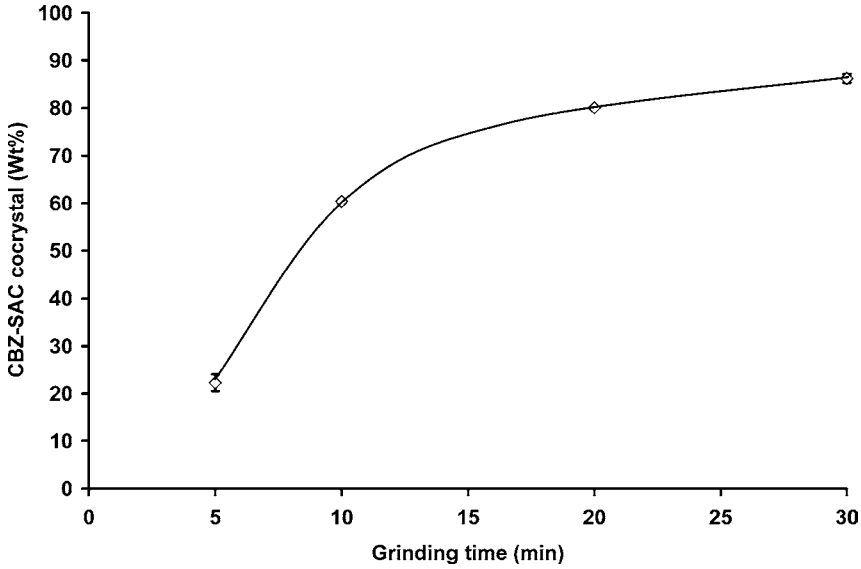

Fig. 6. Cocrystal formation during cogrinding at room temperature.

The T_g values, measured by melt-quenching the reactants in the DSC, are 52°C for anhydrous CBZ (24) and 85°C for SAC. Since the temperature in the cryogenic mill is below the glass transition temperature of the blend and individual components by at least 200°C, molecular mobility decreases under these conditions and the amorphous state generated by cogrinding is maintained (45). This explains the high degree of disorder observed in the XRPD pattern of the equimolar blend of CBZ(III) and SAC after 30 min cogrinding under cryogenic conditions. In contrast, the temperature in the room temperature mill after 30 min cogrinding was observed to rise to 45°C which is close to the glass transition temperatures of CBZ and the coground equimolar blend. Under these conditions, molecular mobility increases in the amorphous phases leading to faster crystallization, and in this case cocrystallization of CBZ–SAC.

The extent of cocrystalization during cogrinding at room temperature is shown in Fig. 6. Quantification was done by FTIR analysis as described in the Methods section. These results indicate the quick formation of the CBZ–SAC cocrystal with a faster rate of cocrystallization in the early stages of the process and approximately 85% cocrystal formed after cogrinding for 30 min.

Cocrystal Formation During Storage

Cocrystallization during solid state cogrinding under ambient temperatures has been reported for a number of systems (4,6,8,9,46). However the formation of cocrystals during storage, to our knowledge, has not been reported. Based on the current understanding of amorphization induced by grinding, and considering the factors that affect

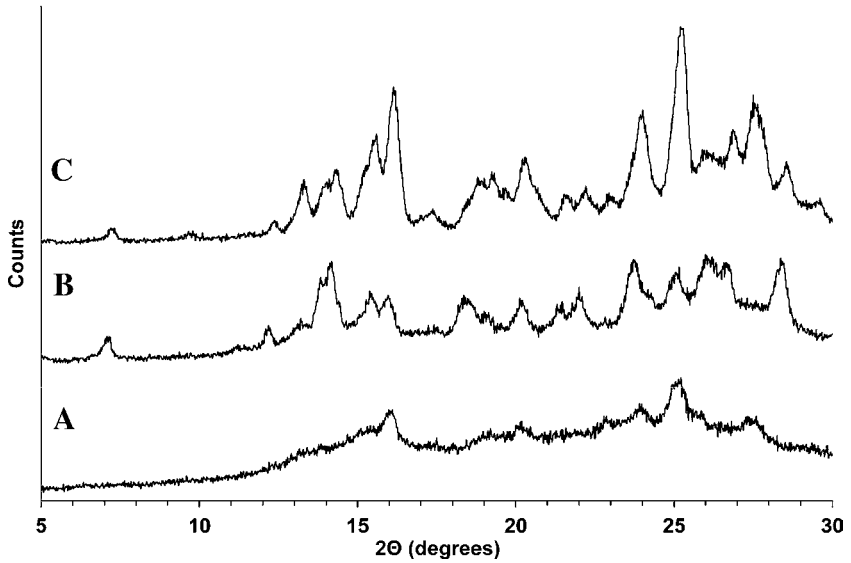

Fig. 7. XRPD patterns showing cocrystal formation during storage after cryogenic cogrinding of CBZ(III) and SAC for 30 min. (A) freshly ground blend (day 0). (B) After storage for 1 day at room temperature and 0%RH. (C) After storage for 1 day at room temperature and 75%RH.

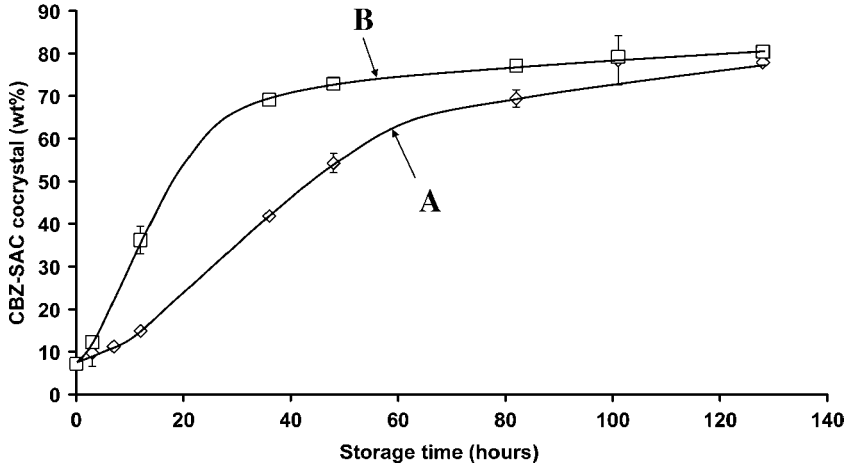

Fig. 8. Cocrystal formation during storage under 0%RH and 75%RH at room temperature after cogrinding CBZ(III) and SAC for 5 min at room temperature. (A) Storage at 0%RH (B) storage at 75%RH.

the stability of amorphous phases and crystallization of single component crystals from the amorphous state, we studied cocrystal formation during storage after cogrinding solid reactants. Coground equimolar blends of CBZ(III) and SAC were stored at room temperature (22 to 25°C) under 0% and 75% RH. Cocrystallization was monitored by XRPD and FTIR.

Figure 7 shows that cocrystallization occurs at 0% and 75% RH after cryogenic cogrinding. Based on these findings we studied the extent of cocrystallization after 5 min ambient temperature cogrinding. Results show that cocrystal formation initiated during cogrinding, proceeds during storage (Fig. 8) and that the rate of cocrystallization increases with RH.

Cocrystal formation during storage after mechanical activation of the solid and the rate dependence on RH suggests an amorphous phase mediated transformation. Water, a potent plasticizer, has a T_g of −138°C and has been shown to decrease the glass transition temperature of amorphous solids (29,30). Therefore, moisture sorption will increase the molecular mobility and the rate of crystallization of amorphous phases. Higher rate of cocrystal formation during storage at high RH may therefore be due to a decrease in T_g and a consequent increase in molecular mobility in the disordered regions of the ground blend.

Cocrystal Formation by Cogrinding Carbamazepine Dihydrate and Saccharin

Since our results indicate that cocrystal formation proceeds through amorphous phases induced by grinding and that the rate of cocrystallization during storage increases on exposure to high relative humidities, one would anticipate that the use of crystalline solvates in cogrinding would increase the rate of cocrystallization. In this case, the solvent in the crystal structure serves as a potent plasticizer. Cogrinding with the dihydrate form of CBZ was therefore carried out to test this hypothesis.

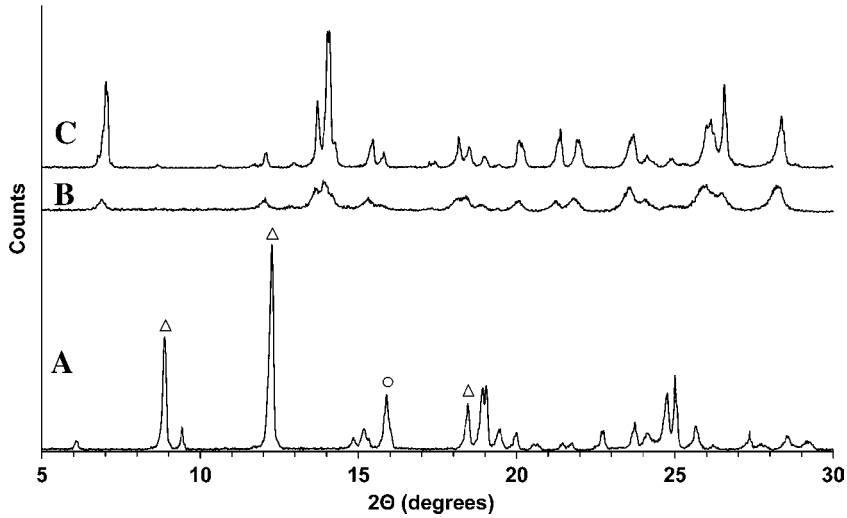

Fig. 9. XRPD pattern showing cocrystal formation after cogrinding CBZ(D) and SAC at room temperature for 10 min. (A) Before cogrinding, (B) after cogrinding and (C) CBZ–SAC cocrystal prepared from solution (symbols △ and ○ indicate CBZ(D) and SAC respectively).

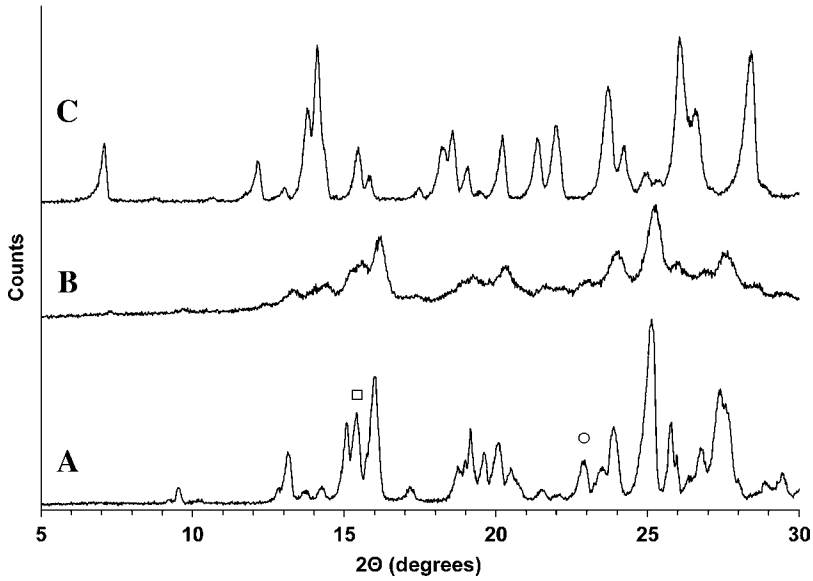

Fig. 10. XRPD pattern of CBZ(III) and SAC showing cocrystal formation after 10 min cogrinding at room temperature. (A) Before cogrinding, (B) after cogrinding and (C) CBZ–SAC cocrystal prepared from solution (symbols □ and ○ indicate CBZ(III) and SAC respectively).

XRPD and FTIR analysis confirm our hypothesis. XRPD patterns (Fig. 9) shows transformation to cocrystal during cogrinding under ambient conditions for 10 min, since the pattern of the coground reactants is in agreement with the pattern of the cocrystal prepared from solution. Peaks characteristic of CBZ(D), CBZ anhydrous polymorphs or SAC were absent after cogrinding.

To compare the rate of cocrystallization between CBZ(D) and CBZ(III) systems, the same cogrinding protocol was used with CBZ(III) and SAC. The XRPD pattern after cogrinding for 10 min (Fig. 10) shows evidence for cocrystal formation and unreacted components.

The FTIR spectra (Fig. 11) provided further evidence for cocrystallization. The spectrum of cocrystal prepared by

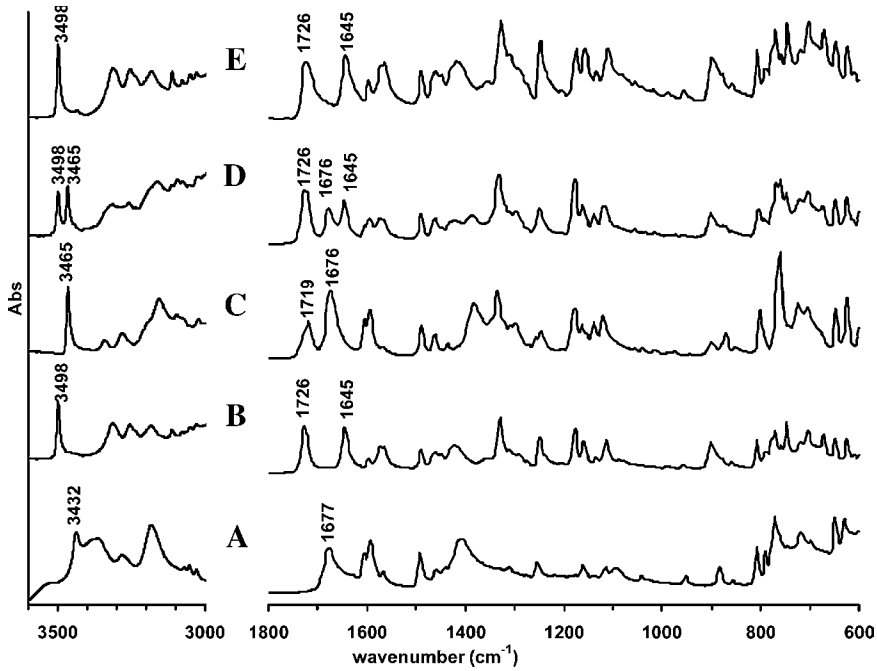

Fig. 11. FTIR spectra showing interactions between CBZ and SAC after 10 min room temperature cogrinding of SAC with either CBZ(D) or CBZ(III). (A) Before cogrinding with CBZ(D), (B) after cogrinding with CBZ(D) (C) before cogrinding with CBZ(III), (D) after cogrinding with CBZ(III), and (E) CBZ–SAC cocrystal from solvent.

cogrinding the dihydrate is very similar to that of the cocrystal prepared from solution. Peaks corresponding to unreacted components were not detected. The spectrum of the coground anhydrous CBZ (III) shows peaks characteristic of cocrystal as well as those corresponding to unreacted CBZ and SAC. These results suggest that the rate of cocrystallization is increased by cogrinding with the hydrated form of CBZ.

The faster rate of cocrystallization by cogrinding with CBZ(D) may be due to the potent plasticizing action of water from the hydrate in reducing the T_g of the amorphous phase. CBZ(D) has 13.5% water and upon dehydration there is 7.9% water in the blend. This leads to significant plasticizing effects, since solvents at low concentrations have the greatest plasticizing effects (29).

Cocrystal Formation in Non-stoichiometric Anhydrous CBZ(III) Blends

Cocrystal formation was observed by cogrinding CBZ(III) and SAC in 1:2 and 2:1 ratios, at ambient temperature for 30 min. The results also suggested the presence of unreacted CBZ and unreacted SAC in the 2:1 and 1:2 blends respectively after cogrinding (results not shown).

DISCUSSION

Our results demonstrate that cocrystal formation during storage is mediated by the formation of disordered regions or amorphous phases induced by cogrinding reactants. The rate of cocrystal formation during cogrinding of solid reactants depends on the grinding temperature and on the solid-state form of the reactants. Cogrinding under cryogenic conditions stabilizes the amorphous phase by lowering the molecular mobility and as a result decreases the rate of cocrystal formation. Amorphization by low temperature grinding (4°C and cryogenic conditions) has been demonstrated for indomethacin (T_g of 43°C) (23,27), while grinding in the proximity of the T_g yielded partially amorphous materials (27).

Studies on the solid-state complexation of coground mixtures of cholic acid with either methyl p-hydroxybenzoate or ibuprofen demonstrated the formation of crystalline inclusion complexes during room temperature grinding and the formation of an amorphous phase under cryogenic conditions (25). The amorphous phase transformed to the crystalline complex after 1 h of heat treatment at 60°C. This process was suggested to be a result of two factors: (1) amorphous phase formation by mechanical force and (2) crystallization of complex by thermal activation. This behavior is similar to that observed in our studies with CBZ and SAC, however, we observed crystallization of the complex occurred at room temperature.

Studies on cogrinding of ursodeoxycholic acid (UDCA) with anthrone and/or phenanhrene exhibited different behavior (26). In these studies, formation of crystalline complex between UDCA and phenanthrene or anthrone was observed during cogrinding at ambient temperature, whereas cogrinding at low temperatures (0°C, −55°C and −70°C) induced amorphization in UDCA while the second component remained crystalline. Heating the mixture of amorphous UDCA and crystalline anthrone and/or crystalline phenanthrene at 75°C for 40 min formed a mixture of the single component crystalline phases. Thus, cocrystallization may be a result of molecular mobility in the amorphous state coupled with favorable interactions between heteromeric molecular complexes, so that crystallization of the pure phases is prevented.

The rate of cocrystal formation during cogrinding, besides depending on the grinding temperature, also depends on the solvated crystal form of reactants. The faster rate of cocrystal formation by cogrinding CBZ(D) and SAC suggests that water in the crystal lattice of CBZ(D) acts as a plasticizer. Matsuda *et al.* (28) have shown that CBZ(D) forms an amorphous phase upon dehydration before conversion to the anhydrous CBZ(III) during grinding at room temperature. Water from CBZ(D) may thus be present in the amorphous phase formed during cogrinding and serves as a plasticizer to reduce the T_g. The predicted T_g for the blend in the presence of this water is at least 20°C below room temperature. The T_g was calculated from the modified Gordon Taylor equation and the Simha–Boyer rule (47) using the following values: T_g of CBZ/SAC blend of 41°C, T_g of water −138°C and K value of 0.35 generally found for small molecules (29). Similar behavior has been reported for crystallization of indomethacin polymorphs during grinding of its solvates (23). We are currently studying the reactivity of solvates under cryogenic conditions.

Cocrystal formation during storage and its dependence on relative humidity demonstrates that moisture facilitates cocrystallization in blends ground under ambient and cryogenic conditions. This behavior is explained by the effect of water on molecular mobility and is consistent with the increased transformation to cocrystal during cogrinding of the hydrated form of CBZ as discussed above.

The formation of CBZ–SAC cocrystal during cogrinding or during storage of mechanically activated blends in preference to the formation of crystalline CBZ and/or SAC raises an interesting question regarding competition between the kinetics of cocrystal formation and crystallization of the individual components from the disordered state. At the molecular level this may be regarded as a competition between heteromeric and homomeric interactions. The formation of CBZ–SAC cocrystal from the amorphous phase suggests that under the conditions in which the experiments were performed heteromeric interactions are favored over homomeric interactions. Similar mechanisms are used in the stabilization of amorphous phases of drugs. Hydrogen bond directed stabilization of amorphous phases with drugs has been demonstrated for amorphous molecular dispersions with polymers (48,49) and from amorphous dispersions with granules of adsorbent (50). In these cases, crystallization of the homomeric drug crystals is prevented by heteromeric interactions with the polymers or the adsorbents.

Comparison of the FTIR spectra after cogrinding under ambient and cryogenic conditions shows that heteromeric aggregation occurs in the disordered state and at low temperatures, although at a slower rate than that at ambient temperature conditions. Similarly, the formation of cocrystal by cogrinding CBZ(D) and SAC suggests that molecular associations between CBZ and SAC resulting in cocrystal are more favored than those observed between CBZ and water in carbamazepine dihydrate.

The thermodynamic stability of the cocrystal with respect to the individual component crystal phases needs to be considered, and is currently being studied in our laboratory. Based on the results presented here, it appears that at room temperature the CBZ–SAC cocrystal is the thermodynamically stable phase.

CONCLUSIONS

The results of this study show that amorphous phases generated during cogrinding can lead to cocrystal formation during storage. Water has a significant effect and increases the rate of cocrystallization during (1) cogrinding hydrated form of reactants, and (2) storage of co-ground reactants at high RH. This study demonstrates that amorphous phases lead to cocrystal formation under conditions where there is increased molecular mobility, and when hydrogen bond associations between different components are more favorable than those between similar components. Perhaps the most relevant implication of these findings is that cocrystals can be formed during pharmaceutical unit operations and during storage. Therefore, transformations to cocrystal may be added to the list of process-induced transformations to consider besides the well-documented transformations involving polymorphs and solvates.

ACKNOWLEDGMENTS

We acknowledge Bei Huang for technical assistance with XRPD and FTIR analysis. We gratefully acknowledge funding from Pfizer, Inc., Ann Arbor, MI, and from the Purdue/Michigan Consortium on the Physical and Chemical Stability of Pharmaceutical Solids.

REFERENCES

1. C. B. Aakeroy and D. J. Salmon. Building co-crystals with molecular sense and supramolecular sensibility. *Cryst. Eng. Comm.* **7**:439–448 (2005).
2. G. Bettinetti, M. Caira, A. Callegari, M. Merli, M. Sorrenti, and C. Tadini. Structure and solid-state chemistry of anhydrous and hydrated crystal forms of the trimethoprim–sulfamethoxypyridazine 1:1 molecular complex. *J. Pharm. Sci.* **89**:478–488 (2000).
3. M. R. Caira. Molecular complexes of sulfonamides. 2. 1/1 complexes between drug molecules — sulfadimidine acetylsalicylic acid and sulfadimidine-4-aminosalicylic acid. *J. Crystallogr. Spectrosc. Res.* **22**:193–200 (1992).
4. M. R. Caira, L. R. Nassimbeni, and A. F. Wildervanck. Selective formation of hydrogen bonded cocrystals between sulfonamide and aromatic carboxylic acids in the solid state. *J. Chem. Soc., Perkin Trans.* **2**:2213–2216 (1995).
5. G. R. Desiraju. Hydrogen bridges in crystal engineering: interactions without borders. *Acc. Chem. Res.* **35**:565–573 (2002).
6. M. C. Etter. Hydrogen bonds as design elements in organic chemistry. *J. Phys. Chem.* **95**:4601–4610 (1991).
7. M. C. Etter and G. M. Frankenbach. Hydrogen-bond directed cocrystallization as a tool for designing acentric organic solids. *Chem. Mater.* **1**:10–12 (1989).
8. M. C. Etter and S. M. Reutzel. Hydrogen-bond directed cocrystallization and molecular recognition properties of acyclic imides. *J. Am. Chem. Soc.* **113**:2586–2598 (1991).
9. M. C. Etter, S. M. Reutzel, and C. G. Choo. Self-organization of adenine and thymine in the solid state. *J. Am. Chem. Soc.* **115**:4411–4412 (1993).
10. M. C. Etter, Z. Urbanczyk-Lipkowska, M. Zia-Ebrahimi, and T. W. Panunto. Hydrogen bond directed cocrystallization and molecular recognition properties of diarylureas. *J. Am. Chem. Soc.* **112**:8415–8426 (1990).
11. A. Nangia and G. R. Desiraju. Supramolecular structures — reason and imagination. *Acta Crystallogr.* **A54**:934–944 (1998).
12. B. Rodríguez-Spong, C. P. Price, A. Jayasankar, A. J. Matzger, and N. Rodríguez-Hornedo. General principles of pharmaceutical solid polymorphism: a supramolecular perspective. *Adv. Drug Deliv. Rev.* **56**:241–274 (2004).
13. N. Rodríguez-Hornedo, S. J. Nehm, and A. Jayasankar. Cocrystals: Design, Properties and Formation Mechanisms, Encyclopedia of Pharmaceutical Technology, 2006 (in press).
14. B. Rodríguez-Spong. Enhancing the Pharmaceutical Behavior of Poorly Soluble Drugs Through the Formation of Cocrystals and Mesophases, Ph.D. Thesis, University of Michigan, 2005.
15. B. Rodríguez-Spong, P. Zocharski, J. Billups, J. McMahon, M. J. Zaworotko, and N. Rodríguez-Hornedo. Enhancing the Pharmaceutical Behavior of Carbamazepine Through the Formation of Cocrystals. *AAPS J.* **5**:Abstract M1298 (2003).
16. A. V. Trask, W. D. S. Motherwell, and W. Jones. Pharmaceutical cocrystallization: engineering a remedy for caffeine hydration. *Cryst. Growth Des.* **5**:1013–1021 (2005).
17. V. R. Pedireddi, W. Jones, A. P. Chorlton, and R. Docherty. Creation of crystalline supramolecular arrays: a comparison of co-crystal formation from solution and by solid state grinding. *Chem. Commun.* **8**:987–988 (1996).
18. A. V. Trask, W. D. S. Motherwell, and W. Jones. Solvent-drop grinding: green polymorph control of cocrystallisation. *Chem. Commun.* **7**:890–891 (2004).
19. S. L. Morissette, Ö. Almarsson, M. L. Peterson, J. F. Remenar, M. J. Read, A. V. Lemmo, S. Ellis, M. J. Cima, and C. R. Gardner. High-throughput crystallization: polymorphs, salts, cocrystals and solvates of pharmaceutical solids. *Adv. Drug Deliv. Rev.* **56**:275–300 (2004).
20. S. J. Nehm, N. Rodríguez-Hornedo, and B. Rodríguez-Spong. Phase solubility diagrams of cocrystals are explained by solubility product and solution complexation. *Cryst. Growth Des.* **6**:592–600 (2005).
21. N. Rodríguez-Hornedo, S. J. Nehm, K. F. Seefeldt, Y. Pagan-Torres, and C. J. Falkiewicz. Reaction crystallization of pharmaceutical molecular complexes. *Mol. Pharmacol.* **3**:362–367 (2006).
22. M. C. Etter, G. M. Frankenbach, and D. A. Adsmond. Using hydrogen bonds to design acentric organic materials for nonlinear optical users. *Mol. Cryst. Liq. Cryst.* **187**:25–39 (1990).
23. K. J. Crowley and G. Zografi. Cryogenic grinding of indomethacin polymorphs and solvates: assessment of amorphous phase formation and amorphous phase physical stability. *J. Pharm. Sci.* **91**:492–507 (2002).
24. D. Murphy, F. Rodríguez-Cintron, B. Langevin, R. C. Kelly, and N. Rodríguez-Hornedo. Solution-mediated phase transformation of anhydrous to dihydrate carbamazepine and the effect of lattice disorder. *Int. J. Pharm.* **246**:121–134 (2002).
25. T. Oguchi, Y. Tozuka, T. Hanawa, M. Mizutani, N. Sasaki, S. Limmatvapirat, and K. Yamamoto. Elucidation of solid-state complexation in ground mixtures of cholic acid and guest compounds. *Chem. Pharm. Bull.* **50**:887–891 (2002).
26. T. Oguchi, K. Kazama, T. Fukami, E. Yonemochi, and K. Yamamoto. Specific complexation of ursodeoxycholic acid with guest compounds induced by co-grinding. II. Effect of grinding temperature on the mechanochemical complexation. *Bull. Chem. Soc. Jpn.* **76**:515–521 (2003).
27. M. Otsuka, T. Matsumoto, and N. Kaneniwa. Effect of environmental temperature on polymorphic solid-state transformation of indomethacin during grinding. *Chem. Pharm. Bull.* **34**:1784–1793 (1986).
28. M. Otsuka, T. Ofusa, and Y. Matsuda. Effect of environmental humidity on the transformation pathway of carbamazepine polymorphic modifications during grinding. *Colloids Surf. B Biointerfaces* **13**:263–273 (1999).

29. B. C. Hancock and G. Zografi. The relationship between the glass transition temperature and the water content of amorphous pharmaceutical solids. *Pharm. Res.* **11**:471–477 (1994).
30. V. Andronis, M. Yoshioka, and G. Zografi. Effects of sorbed water on the crystallization of indomethacin from the amorphous state. *J. Pharm. Sci.* **86**:346–351 (1997).
31. S. G. Fleischman, S. S. Kuduva, J. A. McMahon, B. Moulton, R. D. B. Walsh, N. Rodríguez-Hornedo, and M. J. Zaworotko. Crystal engineering of the composition of pharmaceutical phases: multiple-component crystalline solids involving carbamazepine. *Cryst. Growth Des.* **3**:909–919 (2003).
32. A. Jayasankar, A. Somwangthanaroj, B. Sirinutsomboon, Z. J. Shao, and N. Rodríguez-Hornedo. Cocrystal formation by solid-state grinding and during storage. *AAPS J.***6**:R6159 (2004).
33. K. Seefeldt, J. Miller, S. Ding, and N. Rodríguez-Hornedo. Crystallization of carbamazepine–nicotinamide cocrystal from the amorphous phase. *AAPS J.***6**:R6172 (2004).
34. F. E. M. O'Brien. The control of humidity using saturated salt solutions. *J. Sci. Instrum.* **25**:73–76 (1948).
35. A. Salari and R. E. Young. Application of attenuated total reflectance FTIR spectroscopy to the analysis of mixtures of pharmaceutical polymorphs. *Int. J. Pharm.* **163**:157–166 (1998).
36. A. D. Patel, P. E. Luner, and M. S. Kemper. Quantitative analysis of polymorphs in binary and multi-component powder mixtures by near-infrared reflectance spectroscopy. *Int. J. Pharm.* **206**:63–74 (2000).
37. R. Nair, N. Nyamweya, S. Gonen, L. J. Martinez-Miranda, and S. W. Hoag. Influence of various drugs on the glass transition temperature of poly(vinylpyrrolidone): a thermodynamic and spectroscopic investigation. *Int. J. Pharm.* **225**:83–96 (2001).
38. N. B. Colthup, L. H. Daly, and S. E. Wiberley. *Introduction to Infrared and Raman Spectroscopy*, Harcourt Brace, Boston, 1990.
39. D. W. Mayo, F. A. Miller and R. W. Hannah. *Course Notes on the Interpretation of Infrared and Raman Spectra*, Wiley, Hoboken, NJ, 2004.
40. Y. Hase. The infrared and Raman spectra of phthalimide, N–D-phthalimide and potassium phthalimide. *J. Mol. Struct.* **48**:33–42 (1978).
41. G. Jovanovski. Metal saccharinates and their complexes with N-donor ligands. *CCACAA* **73**:843–868 (2000).
42. S. M. Teleb. Spectral and thermal studies of saccharinato complexes. *J. Argent. Chem. Soc.* **92**:31–40 (2004).
43. G. Jovanovski, S. Tanceva, and B. Soptrajanov. The SO_2 stretching vibrations in some metal saccharinates: spectra–structure correlations. *Spectrosc. Lett.* **28**:1095–1109 (1995).
44. R. J. Behme and D. Brooke. Heat of fusion measurement of a low melting polymorph of carbamazepine that undergoes multiple-phase changes during differential scanning calorimetry analysis. *J. Pharm. Sci.* **80**:986–990 (1991).
45. B. Hancock, S. Shamblin, and G. Zografi. Molecular mobility of amorphous pharmaceutical solids below their glass transition temperatures. *Pharm. Res.* **12**:799–806 (1995).
46. A. Trask and W. Jones. Crystal engineering of organic cocrystals by the solid-state grinding approach. *Top. Curr. Chem.* **254**:41–70 (2005).
47. H. A. Schneider. The Gordon–Taylor equation. Additivity and interaction in compatible polymer blends. *Makromol. Chem.* **189**:1941–1955 (1988).
48. P. Tong and G. Zografi. A study of amorphous molecular dispersions of indomethacin and its sodium salt. *J. Pharm. Sci.* **90**:1991–2004 (2001).
49. L. S. Taylor and G. Zografi. Spectroscopic characterization of interactions between PVP and indomethacin in amorphous molecular dispersions. *Pharm. Res.* **14**:1691–1698 (1997).
50. M. K. Gupta, A. Vanwert, and R. H. Bogner. Formation of physically stable amorphous drugs by milling with neusilin. *J. Pharm. Sci.* **92**:536–551 (2003).